SSRG International Journal of Civil Engineering
ISSN: 2348-8352/ https://doi.org/10.14445/23488352/IJCE-V11I6P112

Volume 11 Issue 6, 107-119, June 2024

Original Article

In-Plane Vibration Analysis of a Multi-Cable-Stayed Beam Carrying Concentrated Masses and the Impact of Thermal Effects

Mohamed Rjilatte[1], Ahmed Adri[2], Omar Outassafte[3], Issam El Hantati[4], Yassine El Khouddar[5], Mohamed Berjal[6], Rhali Benamar[7]

[1,2,3,6]*Laboratory of Mechanics Production and Industrial Engineering (LMPGI), High School of Technology (ESTC), Hassan II University, Casablanca, Morocco.*
[4]*Laboratory for control and mechanical characterization of materials and structures (LCMCMS), National Higher School for Electricity and Mechanics (ENSEM), Hassan II University, Casablanca, Morocco.*
[5]*Engineering of Complex Systems and Structures (ECSS), National Higher School of Arts and Crafts (ENSAM), Moulay Ismail University, Meknes, Morocco.*
[7]*Simulation Studies and Research Laboratory, Instrumentation and Measurements (LERSIM), Mohammadia School of Engineers (EMI), Mohammed V University, Rabat, Morocco.*

[1]*Corresponding Author : mohamed.rjilatte.doc22@ensem.ac.ma*

Received: 16 April 2024 Revised: 26 May 2024 Accepted: 14 June 2024 Published: 30 June 2024

Abstract *- In this paper, we proposed a linear model to analyze the transverse vibrations in the plane of a beam suspended by cables. We conducted a dynamic study of this structure, and the results of the frequencies, as well as the mode shapes of the beam, were obtained. We began our methodology by introducing the equations of motion, which were established at various intervals in the plane of the system, along with their boundary and continuity conditions. Subsequently, we iteratively solved the generalized transcendental frequency equation using the Newton-Raphson method. Once our results were validated by existing literature, we continued our analysis by conducting a parametric study. Masses at different positions and with different values were added, along with a thermal load. We obtained the numerical results of the dynamic study for different positions of the added masses and different values of the thermal load. Through this method, we were able to gain a thorough understanding of the dynamic behavior of the structure in different situations.*

Keywords *- Cable-stayed beam, Linear frequencies.*

1. Introduction

Cable-stayed beams play a crucial role in contemporary engineering, offering sophisticated and high-performance solutions for bridges. They provide the ability to span long distances while reducing the use of massive supports, which is crucial for minimizing environmental impact and construction costs. This innovative solution is perfectly illustrated by cable bridges, which stand out from conventional bridges by their ability to distribute weight thanks to cables attached to the towers. It is essential to conduct a thorough analysis of traffic loads, permanent loads, and climatic and dynamic loads associated with vehicle movement in the design and construction of cable bridges. The interaction between cable and beam models is carefully examined to ensure their longevity and long-term safety. In order to have an in-depth understanding of the complex interactions between the structural elements of cable-stayed bridges, special attention is paid to vibrations both in situ and out of the plane. Using a multi-cable beam model, Cong et al. [1] examined these interactions by assessing the impact of cable mass, rigidity, and flattening ratios on vibration modes. Using differential equations to model the system, Fujino et al. [2] contributed by focusing on nonlinear vibrations caused by variations in cable length and tension. Under different conditions of excitation, P. Warnitchai et al. [3] and Xia et Fujino [4] continued to study auto-parametric vibrations and their linear and nonlinear interactions. The transfer matrix method was used by Su et al. [5] to analyze in detail the free vibrations in the plane, while Li et al. [6] and El Ouni et al. [7] were interested in the effects of wind and earthquakes on the dynamics of cables. Ma's research [8] examined in detail the consequences of cable vibrations, comparing different methods of modeling. Guattuli et al. [9, 10] and Guattuli et Lepidi [11, 12] studied the links between cables and beams, highlighting the impact of moving loads and internal resonance on the dynamic responses of cables.

Author previously investigated the effects of a point mass on clamped beams, employing analytical methods and parametric studies to examine how the mass location influences beam frequencies and mode shapes while also exploring the impact of geometrical non-linearity. Author delved into the geometrically non-linear vibrations of fully clamped, multi-stepped beams carrying multiple masses. Utilizing Euler-Bernoulli beam theory and Von Karman assumptions, these studies derived expressions for kinetic and strain energy, reduced the problem to a non-linear algebraic system through Hamilton's principle, and conducted parametric studies to assess nonlinearity effects on dynamic behavior. Author studied the influence of environmental elements on the dynamics of beams, highlighting the influences of humidity and temperature on vibrations. Aloupis et al. [13] examined how to identify damage in cable-stayed bridges by analyzing the distribution of dead and thermal loads. They proposed digital techniques to simulate damage and study its impact on the structural characteristics of the bridge. Zhang et al. [14] used the D'Alembert principle to analyze the vibration modes and frequencies of suspended bridges, especially those with three pillars. They addressed how these theoretical approaches can be applied to more accurately predict the dynamic behavior of bridges and proposed comparative analysis with concrete examples of engineering.

The research conducted by Cunha et al. [15] and Ren et al. [16] provides a comprehensive vision by addressing various topics such as aerodynamic stability, seismic design, and modal analysis methods to improve the performance of cables. Abdel-Ghaffar and Khalifa [17] focused on the consequences of various forms of cable movement, such as oscillations and vertical movements, on the dynamic characteristics of cable-stayed bridges. They emphasized the need to take these dynamics into account in structural analysis and design in order to improve bridge earthquake resistance. Another research by Nazmy and Abdel-Ghaffar on the analysis of the three-dimensional seismic response of cable-stayed bridges has been deepened [18], focusing on the impact of multi-support seismic excitations. They proposed an in-depth methodological approach to grasp the impact of non-uniform excitations on bridge dynamics and suggested specific analysis methods for practical engineering applications. Subsequent publications, such as those by Cong et al. [19] and Wilson et Gravelle [20], have extended the analysis of damage and response to seismic events, thus providing methodological advice for design.

Other publications highlight structures suitable for cable-stayed bridges, such as the author, who studied free and forced vibrations in shallow arches, taking into account geometric non-linearity. These works, using equations based on Euler-Bernoulli's theory, enable a deeper understanding of the dynamic characteristics of arch structures essential for the design of bridges.

All these studies highlight the importance of dynamic interactions in cable-stayed bridges and suspended structures. In this study, we present a linear model to study transverse vibrations in the plane of a beam suspended by cables. We were able to understand the dynamic behavior of the structure using concentrated masses and added thermal loads through a detailed parametric study. Numerical results on the dynamic behavior of the structure in different situations were obtained by introducing the motion equations and iteratively solving the generalized transcendental frequency equation using the Newton-Raphson method, validating the results against the existing literature. Subsequently, a parametric analysis was performed by adding masses at different locations with a temperature load. This allowed us to observe the behavior of this structure under various loads and situations, which prepared a thorough study to solve other phenomena, including geometrically nonlinear vibrations.

2. Problem Formulation

The cable-stayed beam, composed of several cables attached to two rigid towers, forms a structure where each cable is fixed at both the upper end of each tower and the beam itself. This setup divides the beam into segments defined by the junctions S_j. The static equilibrium configuration of this beam is described by the displacements of the cables U_{cj}, V_{cj}, W_{cj} $(j = 1, 2, \ldots, n)$ and the transverse displacements of the beam $V_{bi} (i = 1, 2, \ldots, n)$. as illustrated in Figure 1. The deformation of the cables follows a parabolic curve due to the small ratio between height D_{cj} and length l_{cj} less than 1/10.

$$Y_{cj} = 4D_{cj}\left(\frac{X_{cj}}{l_{cj}} - \left(\frac{X_{cj}}{l_{cj}}\right)^2\right) \quad (1)$$

Since the axial stiffness of the beam is much greater than that of the cables, the axial movement of the beam can be neglected. The towers are assumed to be rigid, and vibrations minimal, validated by experiments and finite element analyses. The properties of the beam material, such as Kevlar, are critical in the context of mass and temperature. Kevlar's relatively low thermal conductivity simplifies heat transfer, often modeled by the equation:

$$k\frac{d^2T}{dz^2} = 0 \quad (2)$$

Where k represents the thermal conductivity of Kevlar, the solution to this equation shows that the temperature remains constant or varies linearly within the material. The assumptions considered for modeling this beam include one-dimensional homogeneous elastic continuity, Lagrange strain of the centerline for the axial extensions of the cables, and neglecting the flexural, torsional, and shear stiffness of the cables. Suppose that x represents the coordinate along the neutral axis of the beam, measured from the right end and that η represents the coordinate of the position of the added mass.

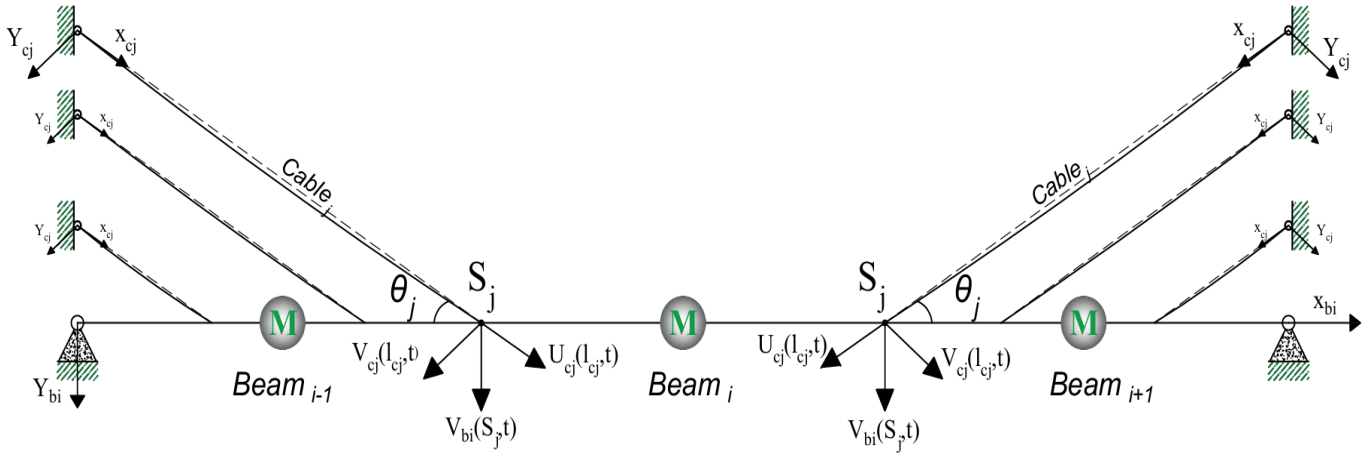

Fig. 1 Configuration of the multi-cable-stayed beam model

Using the above assumptions and simplifications and applying the classical Hamilton principle along with the standard condensation procedure, the following equations of in-plane motion, which govern the transverse vibrations of the cable and sub-beam, are obtained.

$$m_{cj}\frac{\partial^2 V_{cj}}{\partial t^2}+\zeta_{cj}\frac{\partial V_{cj}}{\partial t}- \frac{\partial\left[H_{cj}\frac{\partial V_{cj}}{\partial X_{cj}}+E_{cj}A_{cj}\left(\frac{\partial Y_{cj}}{\partial X_{cj}}+\frac{\partial V_{cj}}{\partial X_{cj}}\right)e_{cj}\right]}{\partial X_{cj}}=P_{cj} \tag{3}$$

$$m_{bi}\frac{\partial^2 V_{bi}}{\partial t^2}+\zeta_{bi}\frac{\partial V_{bi}}{\partial t}+E_{bi}I_{vbi}V_{bi}^{iv}=P_{vbi} \tag{4}$$

Where m_{cj}, ζ_{cj}, H_{cj}, E_{cj}, A_{cj}, are the mass per unit length, damping factor, initial tension, Young's modulus and cross-section area of the j-th cable, respectively. m_{bi}, ζ_{bi}, E_{bi}, I_{vbi}. Are the mass per unit length, damping factor, Young's modulus, and the in-plane second-moment inertia of the cross-section of the i-th sub-beam, respectively. $P_{cj}$and P_{vbi} are the in-plane external excitations that are distributed along the cables and beams, respectively. e_{cj} represents the uniform dynamic elongation of the j-th cable, which is expressed as:

$$e_{cj}=V_{cj}(X_{cj},t)\tan\theta+\int_0^{l_{cj}}\left(\frac{\partial Y_{cj}}{\partial X_{cj}}\frac{\partial V_{cj}}{\partial X_{cj}}+\frac{1}{2}\left(\frac{\partial V_{cj}}{\partial X_{cj}}\right)^2\right)dX_{cj} \tag{5}$$

For the multi-cable-stayed beam model, the partial differential equations outlined in Equations (3) and (4) require specific boundary and compliance conditions.

$$\begin{cases} V_{b1}(0,t)=V_{b(n+1)}(l_b,t)=0 \\ V_{bi}(S_j,t)=V_{b(i+1)}(S_j,t) \\ \dfrac{\partial V_{bi}(S_j,t)}{\partial X_{bi}}=\dfrac{\partial V_{b(i+1)}(S_j,t)}{\partial X_{b(i+1)}} \\ U_{cj}(l_{cj},t)\sin\theta_j+V_{cj}(l_{cj},t)\sin\theta_j=0 \\ V_{cj}(0,t)=0 \end{cases} \tag{6}$$

The relevant continuous mechanical conditions at each junction, as described in Equation (9), must be fulfilled. These conditions are derived from the variational process. Q_i and M_i represent the shear forces and bending moments on the left side of the junction while Q_{i+1} and M_{i+1} represent those on the right side. The longitudinal and transverse tension components in the j-th cable are respectively.

$$T_{xj}=E_{cj}A_{cj}e_{cj} \tag{7}$$

$$T_{yj}=H_{cj}\frac{\partial V_{cj}}{\partial X_{cj}}(l_{cj},t)+E_{cj}A_{cj}e_{cj}\left(\frac{\partial Y_{cj}}{\partial X_{cj}}(l_{cj})+\frac{\partial V_{cj}}{\partial X_{cj}}(l_{cj},t)\right) \tag{8}$$

By ensuring the force balance at each junction, the mechanical condition can be obtained.

$$\begin{aligned} &E_{bi}I_{bi}\frac{\partial^3 V_{bi}}{\partial {X_{bi}}^3}(S_j,t)-E_{b(i+1)}I_{b(i+1)}\frac{\partial^3 V_{b(i+1)}}{\partial {X_{b(i+1)}}^3}(S_j,t) \\ &\quad=E_{cj}A_{cj}e_{cj}\sin\theta_j+\left[H_{cj}\frac{\partial V_{cj}}{\partial X_{cj}}(l_{cj},t)+E_{cj}A_{cj}e_{cj}\left(\frac{\partial Y_{cj}}{\partial X_{cj}}(l_{cj},t)+\frac{\partial V_{cj}}{\partial X_{cj}}(l_{cj},t)\right)\right]\cos\theta_j \\ &\frac{\partial^2 V_{bi}}{\partial {X_{bi}}^2}(S_j,t)=\frac{\partial^2 V_{b(i+1)}}{\partial {X_{b(i+1)}}^2}(S_j,t) \\ &\frac{\partial^2 V_{b1}}{\partial {X_{b1}}^2}(0,t)=\frac{\partial^2 V_{b(n+1)}}{\partial {X_{b(n+1)}}^2}(l_b,t) \end{aligned} \tag{9}$$

The initial temperature is assumed to be T_0, while the temperature variation can be uniformly increased to a final value of T, and the temperature difference.

$$\Delta T = T - T_0 \tag{10}$$

The equations of motion for axial and transverse beam vibrations are frequently considered in the literature and have been adopted according to [21] as follows.

$$\frac{\partial N_{X_{bi}}}{\partial X_{bi}} = 0 \tag{11}$$

$$\frac{\partial^2 M_{X_{bi}}}{\partial {X_{bi}}^2} + \frac{\partial}{\partial X_{bi}}\left(N_{X_{bi}} \frac{\partial V_{bi}(X_{bi},t)}{\partial X_{bi}}\right) = I_{vbi} \frac{\partial^2 V_{bi}(X_{bi},t)}{\partial t^2} \tag{12}$$

$N_{X_{bi}}$ Et $M_{X_{bi}}$ are the axial force and bending moment, respectively, acting at the midpoint of the beam. These forces account for the effect of thermal loads and are expressed relative to [22, 23] as follows.

$$\begin{pmatrix} N_{X_{bi}} \\ M_{X_{bi}} \end{pmatrix} = \begin{pmatrix} A_{11} & B_{11} \\ B_{11} & D_{11} \end{pmatrix} \begin{pmatrix} \dfrac{\partial U_{bi}(X_{bi},t)}{\partial X_{bi}} \\ -\dfrac{\partial^2 V_{bi}(X_{bi},t)}{\partial t^2} \end{pmatrix} - \begin{pmatrix} N_{X_{bi}}^T \\ M_{X_{bi}}^T \end{pmatrix} \tag{13}$$

Where $N_{X_{bi}}$ Et $M_{X_{bi}}$ are generated by the temperature change, they are calculated using the formulations given in accordance with [24] as follows.

$$\begin{pmatrix} N_{X_{bi}}^T & M_{X_{bi}}^T \end{pmatrix} = \int_{-H/2}^{H/2} (E\alpha\Delta T)(l, z - z_0)\, dz \tag{14}$$

$$z_0 = \frac{\int_{-H/2}^{H/2} zE\, dz}{\int_{-H/2}^{H/2} E\, dz} \tag{15}$$

Earlier research indicates that asymmetrical bridges are particularly vulnerable to damage because vibration energy tends to focus on fewer cables when the excitation frequencies match the system's natural frequencies corresponding to localized mode shape [25]. Therefore, a symmetrical model was adopted for this study with the assumptions that:

$$m_{bi} = m_b\,, m_{cj} = m_c\,, E_{cj}A_{cj} = E_cA_c\,,\ E_{bi}I_{vbi} = E_bI_b \tag{16}$$

A non-dimensional version of Equations (3) and (4), along with the corresponding boundary conditions, Equations (5) and (9), can be derived by introducing the following variables.

$$\begin{cases} x_{cj} = \dfrac{X_{cj}}{l_{cj}}\ , y_{cj} = \dfrac{Y_{cj}}{l_{cj}}\ , v_{cj} = \dfrac{V_{cj}}{l_{cj}}\ , d_{cj} = \dfrac{D_{cj}}{l_{cj}} \\ \xi_{cj} = \dfrac{\zeta_{cj}}{m_{cj}\omega_0}\ \ , \xi_{bi} = \dfrac{\zeta_{bi}}{m_{bi}\omega_0} \\ x_{bi} = \dfrac{X_{bi}}{l_b}\ , v_{bi} = \dfrac{V_{bi}}{l_b}\ , s_{bi} = \dfrac{S_{bi}}{l_b} \\ \tau = \omega_0 t\ \ , \lambda = \dfrac{N_{X_{bi}}^T}{D_{11}} = \dfrac{N_{x_{bi}}^T}{E_bI_b} \end{cases} \tag{17}$$

Where ω_0 is a specified frequency, like the system's primary in-plane natural frequency, and it can be taken as 1. Additionally, the following dimensionless quantities are defined.

$$\rho = \frac{m_c}{m_b}\ ,\ \mu_{cj} = \frac{E_cA_c}{H_{cj}}\ ,\ \chi = \frac{E_bI_b}{{l_b}^2E_cA_c}\ ,\ \gamma_{cj} = \frac{l_b}{l_{cj}} \tag{18}$$

Furthermore, the following dimensionless spatial frequencies of the cable and sub-beam are introduced.

$$\beta_{bi}{}^4 = \frac{m_b{l_b}^4{\omega_0}^2}{E_bI_b}\ \ ,\ \ \beta_{cj}{}^2 = \frac{m_c{l_{cj}}^2{\omega_0}^2}{H_{cj}}$$
$$\beta_{bi}^2 = \omega\sqrt{\frac{m_bl_b^4}{E_bI_b}}\ \ \ ,\ \ \ \beta_{cj} = \omega\sqrt{\frac{m_cl_{cj}^2}{H_{cj}}} \tag{19}$$

Where ω denotes the dimensional temporal frequencies of the system's in-plane and out-of-plane modal motions, respectively. The relationship between the spatial frequencies of the cable and sub-beam can be derived by solving Equation (19) for ω, and it is expressed as follows.

$$\beta_{vcj} = \beta_{vb}^2\frac{\alpha_j}{\gamma_{cj}} \tag{20}$$

Where α_j is defined as:

$$\alpha_j = \sqrt{\mu_{cj}\rho\chi} \tag{21}$$

By expanding the dimensionless equation of the cable and ignoring the nonlinear and structural damping terms, the linearized self-adjoint boundary value problem of the multi-cable-stayed beam model can be derived using the separation of variables method and the one-dimensional coordinate system, (x), $x_{cj} = x_{bi} = x$

$$-\beta_{vb}^4 w_{vbi} + \frac{\partial^4 w_{vbi}}{\partial x^4} = 0 \tag{22}$$

$$\beta_{vcj}^3 w_{vcj} + \frac{\partial^2 w_{vcj}}{\partial x^2} = 8\mu_{cj}d_{cj}e_{cj} \tag{23}$$

Additionally, the linearized geometric and mechanical boundary conditions can be derived simultaneously and are expressed as follows.

$$w_{vc1}(0) = w_{vc2}(0) = 0,\ w_{vc1}(1) = \gamma_{c1}w_{vb1}(s_1)\cos\theta\,,\ w_{vc2}(1) = \gamma_{c2}w_{vb2}(s_2)\cos\theta$$
$$w_{vb1}(0) = w_{vb3}(1) = \left.\frac{\partial^2 w_{vb1}}{\partial x^2}\right|_{x=0} = \left.\frac{\partial^2 w_{vb3}}{\partial x^2}\right|_{x=1} = 0,\ w_{vb1}(s_1) = w_{vb2}(s_1), \left.\frac{\partial w_{vb1}}{\partial x}\right|_{x=s_1} = \left.\frac{\partial w_{vb3}}{\partial x}\right|_{x=s_2}$$
$$\left.\frac{\partial^2 w_{vb1}}{\partial x^2}\right|_{x=s_1} = \left.\frac{\partial^2 w_{vb2}}{\partial x^2}\right|_{x=s_2}, w_{vb2}(s_2) = w_{vb3}(s_2), \left.\frac{\partial w_{vb2}}{\partial x}\right|_{x=s_2} = \left.\frac{\partial w_{vb3}}{\partial x}\right|_{x=s_2}, \left.\frac{\partial^2 w_{vb2}}{\partial x^2}\right|_{x=s_2} = \left.\frac{\partial^2 w_{vb3}}{\partial x^2}\right|_{x=s_2}$$
$$\chi\left[\left.\frac{\partial^3 w_{vb1}}{\partial x^3}\right|_{x=s_1} - \left.\frac{\partial^3 w_{vb2}}{\partial x^3}\right|_{x=s_1}\right] - \left(\sin\theta + \left.\frac{\partial y_{c1}}{\partial x}\right|_{x=1}\cos\theta_1\right)e_{c1} - \frac{\cos\theta}{\mu}\left.\frac{\partial w_{vc1}}{\partial x}\right|_{x=1} = 0$$
$$\chi\left[\left.\frac{\partial^3 w_{vb2}}{\partial x^3}\right|_{x=s_2} - \left.\frac{\partial^3 w_{vb3}}{\partial x^3}\right|_{x=s_2}\right] - \left(\sin\theta + \left.\frac{\partial y_{c2}}{\partial x}\right|_{x=1}\cos\theta_1\right)e_{c2} - \frac{\cos\theta}{\mu}\left.\frac{\partial w_{vc2}}{\partial x}\right|_{x=1} = 0 \tag{24}$$

Where w_{vcj} and w_{vbi} are modal eigenfunctions is the linearized dynamic elongation of the cable and is expressed as follows.

$$e_{cj} = w_{cj}(1)\tan\theta_j + \int_0^1 \frac{\partial y_{cj}}{\partial X_{cj}} \frac{\partial w_{cj}}{\partial X_{cj}} dx_{cj} \tag{25}$$

The compatibility conditions associated with the added masses are:

$$\begin{gathered} w_{vbi}(x)|_{x=\eta} = w_{vb(i+1)}(x)\big|_{x=\eta} \\ \left.\frac{dw_{vbi}(x)}{dx}\right|_{x=\eta} = \left.\frac{dw_{vbi}(x)}{dx}\right|_{x=\eta}, \quad \left.\frac{d^2w_{vbi}(x)}{dx^2}\right|_{x=\eta} = \left.\frac{d^2w_{vbi}(x)}{dx^2}\right|_{x=\eta} \\ \left.\frac{d^3w_{vbi}(x)}{dx^3}\right|_{x=\eta} = \left.\frac{d^3w_{vbi}(x)}{dx^3}\right|_{x=\eta} + M\,\omega^2 \left.\frac{\partial w_{vbi}(x)}{\partial x}\right|_{x=\eta} \end{gathered} \tag{26}$$

It is widely recognized that the exact closed-form solutions of Equations (x) and (x) take the following form.

$$\begin{aligned} w_{vbi}(x) = A_{bi}\,sin\left(\sqrt{\frac{1}{2}\lambda + \frac{1}{2}\sqrt{\lambda^2 + 4\beta_{vbi}}}(x)\right) + B_{bi}\,cos\left(\sqrt{\frac{1}{2}\lambda + \frac{1}{2}\sqrt{\lambda^2 + 4\beta_{vbi}}}(x)\right) \\ + C_{bi}\,sinh\left(\sqrt{-\frac{1}{2}\lambda + \frac{1}{2}\sqrt{\lambda^2 + 4\beta_{vbi}}}(x)\right) + D_{bi}\,cosh\left(\sqrt{-\frac{1}{2}\lambda + \frac{1}{2}\sqrt{\lambda^2 + 4\beta_{vbi}}}(x)\right) \end{aligned} \tag{27}$$

$$w_{vcj}(x) = E_{cj}\,sin(\beta_{vcj}x) + F_{cj}\,cos(\beta_{vcj}x) + \Delta_{cj} \tag{28}$$

Where,

$$\Delta_{cj} = \frac{8\mu_{cj}d_{cj}e_{cj}}{\beta_{vcj}^2} \tag{29}$$

By manipulating Equations (27) and (28) with the relevant geometrical and mechanical compliance conditions (24) and (26), the following characteristic equation can be obtained:

$$F(\omega)\Lambda = 0 \tag{30}$$

Where $F(\omega)$ is the coefficient matrix. Λ is the vector consisting of coefficients in Equations (x) and (x), which is defined as:

$$\Lambda = \left[\ldots, A_{bi}, B_{bi}, C_{bi}, D_{bi}, \ldots, E_{cj}, F_{cj}, \ldots\right]^T \tag{31}$$

The frequency ω can be determined by setting the determinant of the coefficient matrix $F(\omega)$ in Equation (x) to zero. Once ω is found, the coefficient vector Λ can be readily determined by considering the boundary conditions. The mode functions of each order can then be derived, where the normalization is done such that max. $\{w_{vbi}, w_{vcj}\} = 1$

3. Results and Discussion

3.1. Double-Cable-Stayed Beam Model

The system's numerical solution was achieved using the Newton-Raphson method, implemented in MATLAB. The beam, characterized as homogeneous and isotropic, is fixed at both ends and supported by elastic cables at positions $x = 1/3l_b$ and $= 2/3l_b$, where l_b denotes the beam's total length. This section includes a comparative analysis with findings documented in existing literature prior to addressing the study's main focus: examining the vibrations of beams suspended by two cables while supporting concentric masses. Extensive parametric analysis will be conducted, adjusting variables such as the placement, magnitude, and quantity of masses, as well as a variable thermal load applied to the beam, to explore their impact on the amplitudes and frequencies of linear vibrations. The numerical solution of the system was obtained using MATLAB, where the Newton-Raphson algorithm was employed to solve the equations derived from the establishment of the boundary conditions and continuity conditions. To verify the linearized dynamic model developed in this study, an asymmetric cable-stayed beam model featuring two identical cables was analyzed. These cables divide the beam into three equal sub-beams at their junctions with the deck beam. The properties assigned to the deck beam are Young's modulus $34.5\,GPa$, cross-sectional moment of inertia $9.8\,m^4$, cross-sectional area $16{,}3\,m^2$, mass per unit length of $4{,}4 \times 10^4\,kg/m$, and the total length $300m$. For the cables, the properties include Young's modulus $210\,GPa$, cross-sectional area $6{,}273 \times 10^{-3}\,m^2$, mass per unit length $10{,}4\,kg/m$, an initial force $1\,Mn$, and an inclination angle of $\pi/6\,rad$. The gravitational acceleration applied in this study is $9.8\,m/s^2$. Table 1 offers a detailed comparison of the frequency values from this study with those referenced in prior literature, highlighting the precision of our current findings. The data demonstrates substantial consistency, with only negligible discrepancies observed in the frequencies of the first ten-mode shapes. This consistency suggests that the

methodologies and analytical approaches used in this research are both effective and dependable, aligning closely with well-established data in the field.

We began our methodology by introducing the equations of motion, which were established at various intervals in the plane of the system, along with their boundary and continuity conditions. Subsequently, we iteratively solved the generalized transcendental frequency equation using the Newton-Raphson method. Once our results were validated by existing literature, the table compares the first 10 natural frequencies of a double-cable-stayed beam model calculated by two different methods: our results against the Finite Element Method (FEM) and the reference values.It shows the natural frequencies for each method, along with the percentage error compared to the reference values. Both methods demonstrate high accuracy, with small errors relative to the reference data.

3.2. Influence of a Single Mass on Frequencies

In this first case study, we examine a beam suspended by two elastic cables fixed at the same position as the double-cable-stayed beam. The suspension configuration is such that the beam supports a single, concentric mass. This mass can vary in intensity and position relative to the beam, allowing us to study different loading scenarios and their impacts on the system.The main objective of this case study is to analyze how variations in the position and intensity of the mass influence the vibrational behavior of the beam. Specifically, we aim to understand how these factors modify the first three dimensionless natural frequencies of the suspended beam. The results presented in Table 2 provide an overview of the variations in vibrational behavior in response to changes in the mass parameters.

Table 1. The first 10 natural frequencies of the double-cable-stayed beam model

Natural frequency	1st	2nd	3rd	4th	5th	6th	7th	8th	9th	10th
Present	0,1366	0,2313	0,4354	0,7849	1,2162	1,3427	1,3428	1,7417	2,3741	2,6855
Ref [1]	0,1355	0,2307	0,4354	0,7848	1,2162	1,3503	1,3503	1,7417	2,3740	2,6854
Error (%)	0,8118	0,2601	0,0000	0,0127	0,0000	-0,5628	-0,5554	0,0000	0,0042	0,0037
FEM	0,1360	0,2307	0,4349	0,7840	1,2147	1,3436	1,3437	1,7391	2,3696	2,6890
Error (%)	0,4412	0,2601	0,1150	0,1148	0,1235	-0,0670	-0,0670	0,1495	0,1899	-0,1302

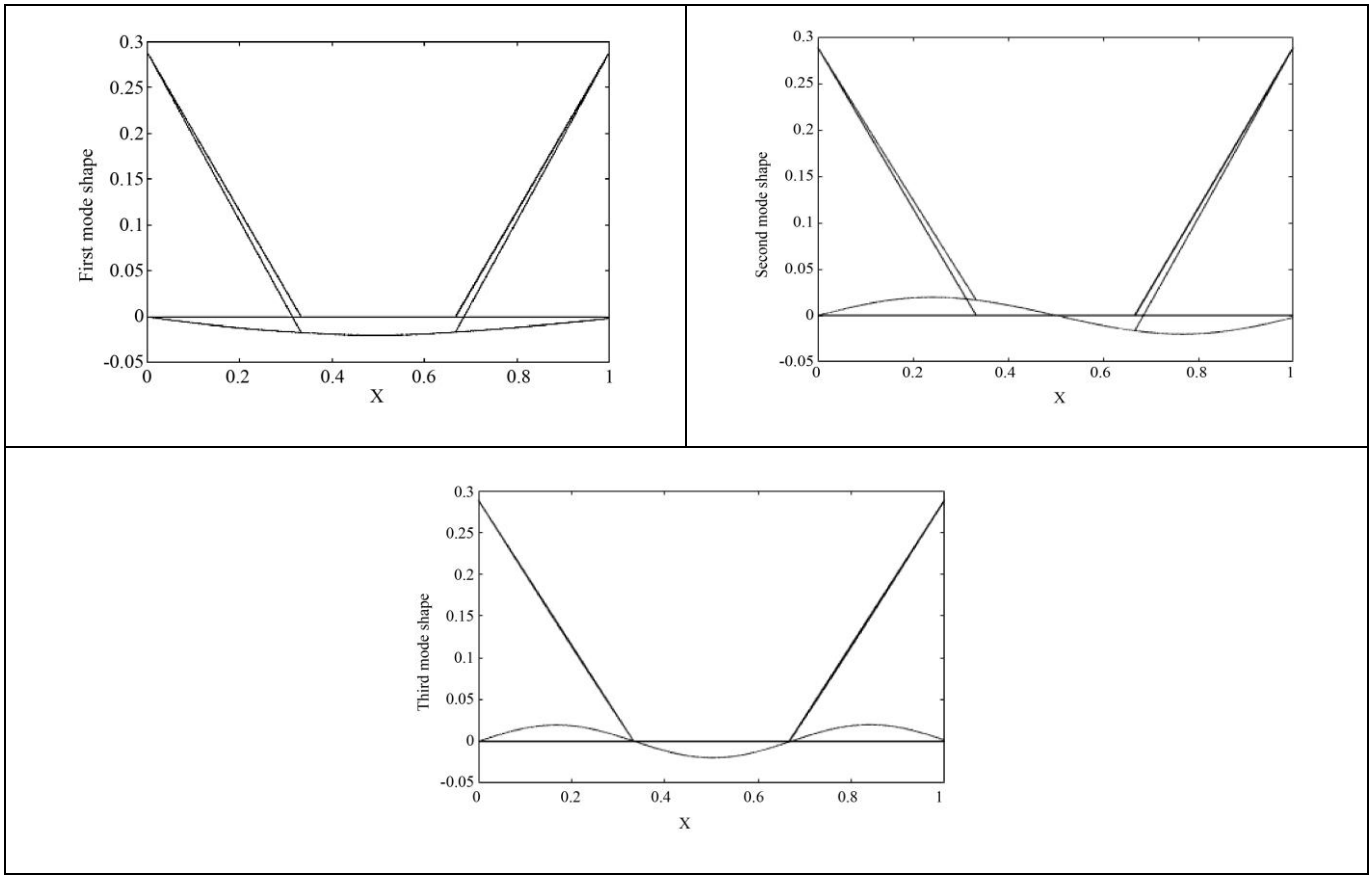

Fig. 2 Presentation of the first three mode shapes of a double-cable-stayed beam model

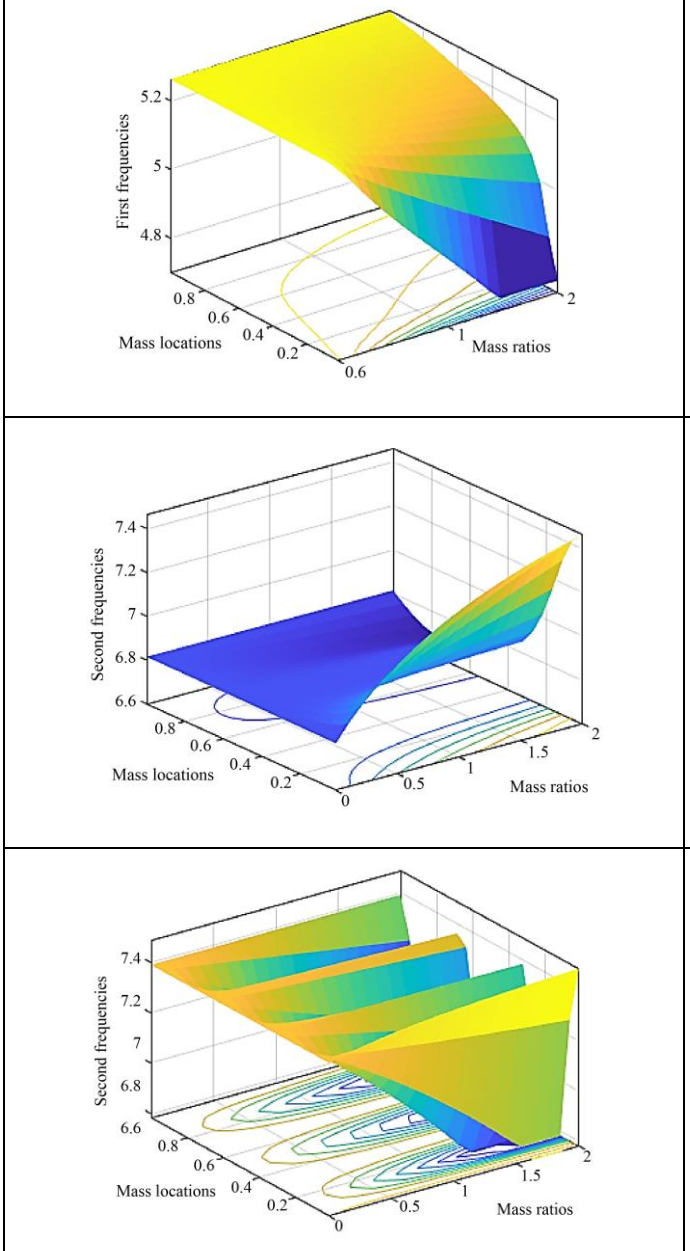

Fig. 3 The variation of the first three dimensionless natural frequencies of a suspended beam is analyzed as a function of the dimensionless mass intensity and the dimensionless position of the mass

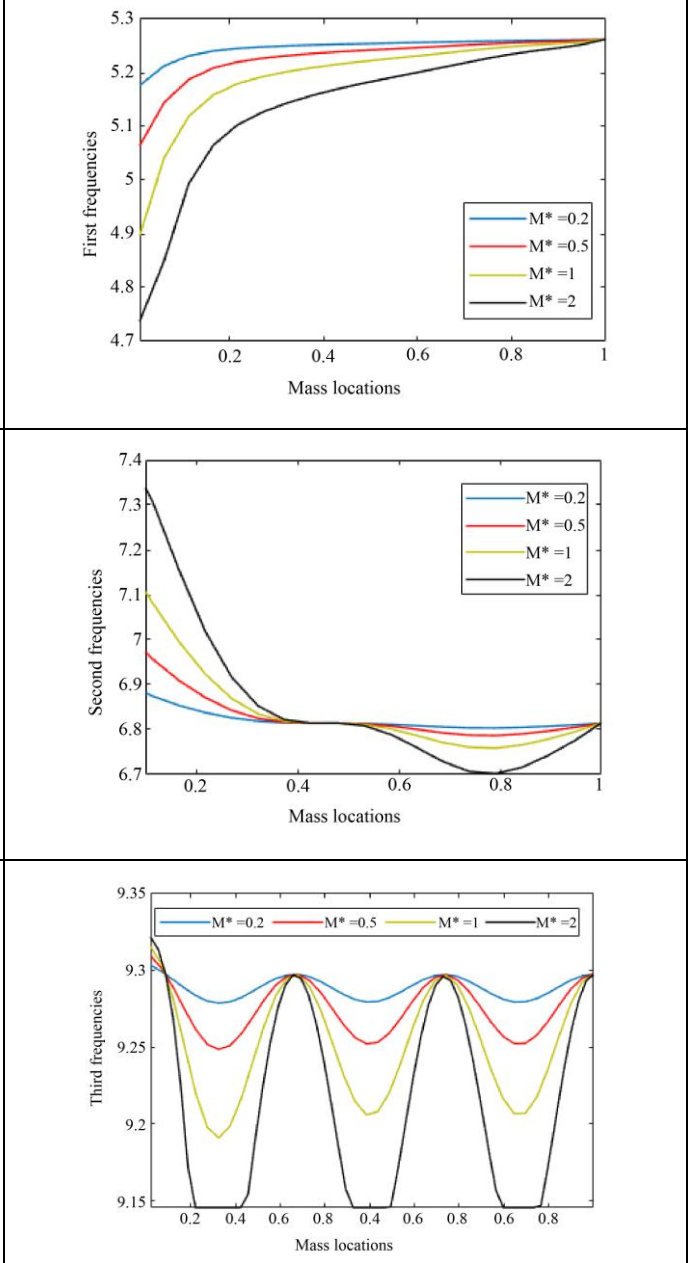

Fig. 4 The representation of the first three dimensionless natural frequencies of a suspended beam is depicted as a function of the dimensionless mass location for various values of dimensionless mass intensity

Figures 3 illustrate how the location of the mass affects the dimensionless frequencies for specific dimensionless intensities of the mass ($M = 0.2, 0.5, 1,$ and 2). It can be seen that the location of the crack changes the dimensionless frequencies of the beam, with frequency oscillations and a decreasing slope as the mass moves from the left end to the right end. These figures show that the frequency varies with the location of the mass, which is due to the fact that the mass has little effect on the vibratory response when it is located at the vibration nodes or inflection points. The effect of the mass on frequencies becomes greater when the mass is further away from these points. In addition, it can be seen that increasing the adimensional intensity of the mass reduces the frequency because this decreases the rigidity of the structure. It can also be seen that for all three modes, the frequencies are lower when the mass is close to the free end of the cantilever beams. In other words, the impact of the mass on the frequency is more significant near the rigid zone of the beam. Figure 4

illustrates that, for all three modes of vibration, the frequencies associated with a given mass intensity oscillate as the position of the mass moves from the fixed end to the other fixed end of the beam. In these figures, the number of oscillations increases with the number of modes, which is due to the fact that the oscillations are relative to the excitation frequency specific to each mode. In addition, the influence of the symmetry of the beam with respect to its central point can be seen in the normalized frequency curves, which are also symmetrical for a fixed beam. Table 2 shows the first three natural frequencies of a cable-stayed system fixed at both ends with a concentrated mass placed at its midpoint. The mass ratio studied ranges from 0 to 2. The results clearly show a reduction in natural frequencies for all three modes as the mass ratio increases. This trend is significant and corroborates the principles of the Rayleigh-Ritz theory, which proposes that the natural frequencies of a structure are inversely proportional to its mass. In practice, this means that adding mass to a system lowers its natural frequencies while removing mass increases them. Understanding this relationship is essential to comprehending how mass affects the dynamic behavior of structural systems. The data shows a clear trend: as the mass intensity increases, the natural frequencies decrease for all three modes. This trend supports the Rayleigh-Ritz theory, which states that natural frequencies are inversely proportional to mass. The position of the added mass also affects the frequencies, but the overall trend of decreasing frequencies with increasing mass intensity remains consistent. This information is crucial for understanding how mass affects the dynamic behavior of structural systems.The effect of mass size is also shown in terms of curvature, as depicted in the figure. By varying the mass from 0 to 2, with this mass in the middle of the beam, we can see that the curvature is at its maximum when the magnitude of the mass is at its maximum. However, the curvature does not change at the ends of the beam.

Table 2. Analysis of the first three dimensionless natural frequencies of a double cable-stayed beam with an added mass at various locations and mass ratios

Mass Intensity	Mass Location	Frequencies of the Beam		
		1	2	3
0.2	0.2	5,2439	6,8430	9,2807
	0.4	5,2523	6,8148	9,2913
	0.6	5,2562	6,8110	9,2912
	0.8	5,2598	6,8036	9,2811
0.5	0.2	5,2170	6,8836	9,2544
	0.4	5,2372	6,8151	9,2820
	0.6	5,2469	6,8059	9,2817
	0.8	5,2556	6,7871	9,2565
1	0.2	5,1737	6,9469	9,2064
	0.4	5,2124	6,8156	9,2667
	0.6	5,2314	6,7974	9,2661
	0.8	5,2489	6,7594	9,2153
2	0.2	5,0922	7,0631	9,1456
	0.4	5,1633	6,8164	9,2370
	0.6	5,2006	6,7811	9,2351
	0.8	5,2348	6,7031	9,1456

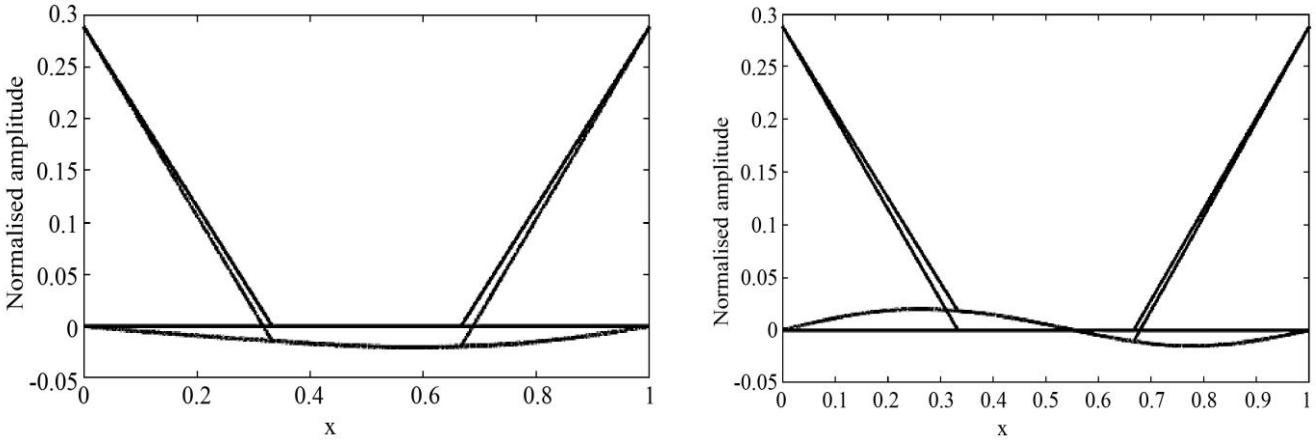

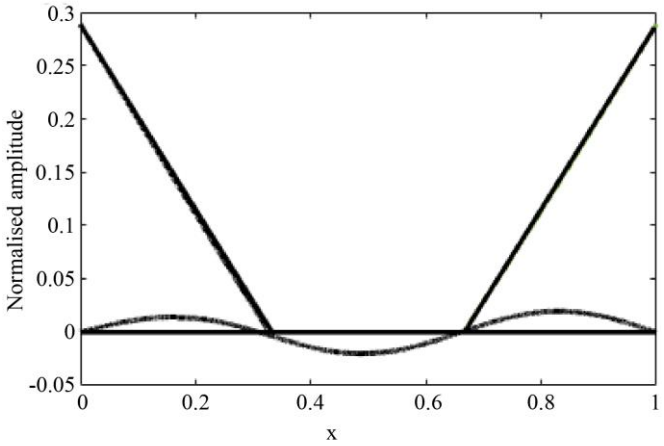

Fig. 5 Presentation of the first three mode shapes of a beam with cables supporting a mass of intensity $M = 2$ at $x = 0.5l_b$

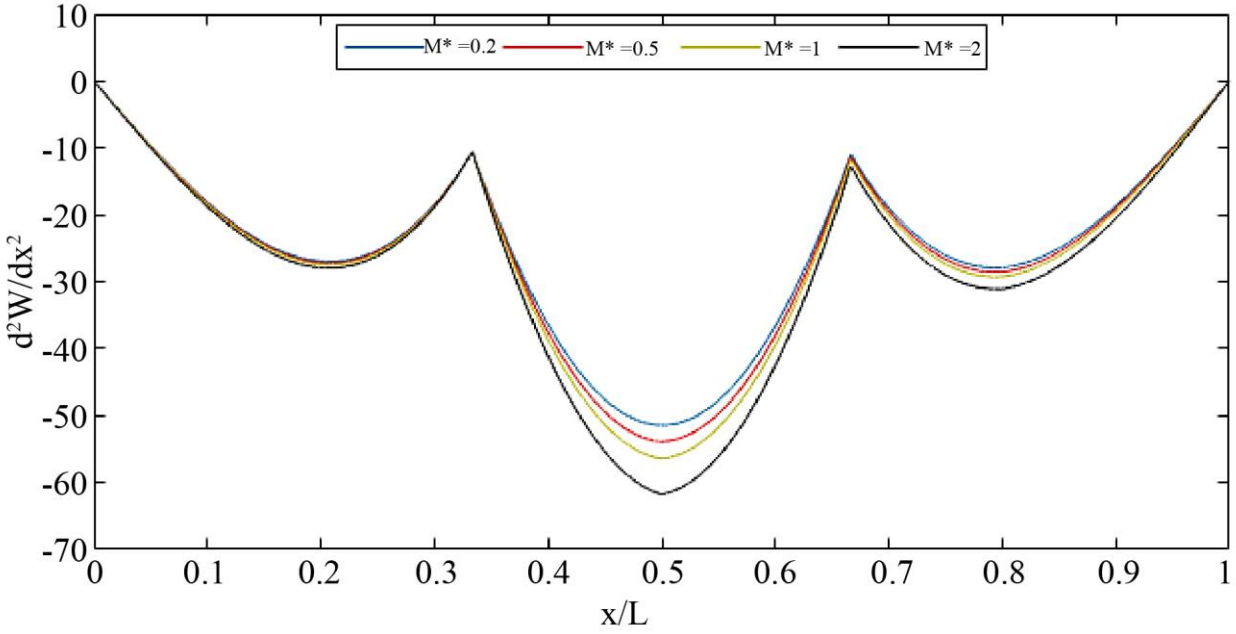

Fig. 6 The curvatures of a cable-stayed beam carrying a concentric mass at the middle, with varying mass magnitudes

Table 3. The first three dimensionless natural frequencies of a beam are supported by two symmetrically positioned cables carrying two masses located symmetrically

Mass Locations	Mass Intensities	Frequencies		
		1	2	3
η =0.2, η =0.8	0.2	5,2577	6,7942	9,2642
	0.5	5,2506	6,7632	9,2126
	1	5,2386	6,7100	9,1456
	2	5,2147	6,5936	9,1456
η =0.4, η =0.6	0.2	5,2500	6,8075	9,2849
	0.5	5,2312	6,7966	9,2661
	1	5,2005	6,7785	9,2351
	2	5,1402	6,7410	9,1742
$\eta = 1/3, \eta = 2/3$	0.2	5,2527	6,7994	9,2973
	0.5	5,2378	6,7761	9,2969
	1	5,2133	6,7368	9,2962
	2	5,1655	6,6533	9,2950

3.3. Influence of Multiple Concentrated Masses on the Frequencies

In this part, we examine how the positions and intensities of multiple concentrated masses influence the natural frequencies of the cable-stayed beam. We establish a relationship between the natural frequency and both the intensity and position of the masses. In this simulation, we vary the intensity of the concentrated mass ratios from 0 to 2.

Table 3 presents the results for the first three dimensionless natural frequencies of a beam supported by two symmetrically positioned cables carrying two masses located symmetrically. Tables 4 to 6 present the values of the first three-dimensional natural frequencies of a beam supporting three concentrated masses, two of which are positioned symmetrically and the other at the middle of the beam.

In this investigation, we vary the position of the two concentrated masses near the ends of the beam, as well as their intensity, to observe their effects on the linear vibratory behavior of the beam. From Tables 3 to 6, it can be concluded that increases in the mass magnitude lead to a decrease in the natural frequencies of the beam. This inverse relationship is due to the added mass increasing the overall inertia of the system, which in turn reduces its ability to oscillate at higher frequencies. The decrease in natural frequencies is particularly significant when the beam supports a higher number of concentrated masses. This is because each additional mass further amplifies the inertia, compounding the effect on the system's dynamic behavior. As more masses are added, the beam becomes less stiff and more prone to lower frequency vibrations.

The effect of varying the mass ratio was also investigated in terms of the curvature of the beam by varying M from 0 to 2, while the other parameters were set as follows: $x = 0.2l_b, 0.5l_b \; et \; 0.8l_b$

Figure 6 shows the obtained curvatures from a beam supporting three concentric masses located at $x = 0.2l_b, 0.5l_b \; et \; 0.8l_b$. The variation in the mass ratios shows a significant effect on the curvatures when the value of M increases from 0 to 2, this effect remains insignificant, especially at the middle.

3.4. Influence of Thermal Loading on the Frequencies

In this section, we investigate the impact of thermal loading on the free vibrations of a beam suspended from a cable.The beam studied in this section supports, in the first case, a single mass at the center with a mass ratio of $M = 0.5$, the results of which are given in Table 7. In the second case, it supports two masses positioned symmetrically at $x = 0.2l_b$ and $x = 0.8l_b$, whose magnitudes are: $M_1 = M_3 = 2$. The effects of these masses on the linear vibration behavior are shown in Table 8.

Table 4. The first three dimensionless natural frequencies of a beam supporting three concentrated masses, two of which are positioned symmetrically and the other at the middle of the beam with $M_2 = 0.5$

Mass Locations	Mass Intensities	Frequencies		
		1	2	3
$\eta = 0.2, \eta = 0.8$	0.2	5,2378	6,7940	9,2165
	0.5	5,2307	6,7629	9,1608
	1	5,2188	6,7097	9,1456
	2	5,1954	6,5932	9,1456
$\eta = 0.4, \eta = 0.6$	0.2	5,2301	6,8072	9,2394
	0.5	5,2116	6,7964	9,2206
	1	5,1810	6,7781	9,1896
	2	5,1211	6,7408	9,1456
$\eta = 1/3, \eta = 2/3$	0.2	5,2327	6,7990	9,2516
	0.5	5,2181	6,7759	9,2513
	1	5,1938	6,7365	9,2505
	2	5,1465	6,6529	9,2491

Table 5. The first three dimensionless natural frequencies of a beam supporting three concentrated masses, two of which are positioned symmetrically and the other at the middle of the beam with $M_2 = 1$

Mass locations	Mass Intensities	Frequencies		
		1	2	3
$\eta = 0.2, \eta = 0.8$	0.2	5,2178	6,7937	9,1674
	0.5	5,2110	6,7625	9,1456
	1	5,1994	6,7093	9,1456
	2	5,1763	6,5928	9,1456
$\eta = 0.4, \eta = 0.6$	0.2	5,2103	6,8069	9,1929
	0.5	5,1920	6,7961	9,1740

	1	5,1617	6,7778	9,1458
	2	5,1023	6,7405	9,1456
$\eta = 1/3, \eta = 2/3$	0.2	5,2128	6,7987	9,2052
	0.5	5,1984	6,7756	9,2047
	1	5,1745	6,7361	9,2038
	2	5,1274	6,6526	9,2022

Table 6. The first three dimensionless natural frequencies of a beam supporting three concentrated masses, two of which are positioned symmetrically and the other at the middle of the beam with $M_2 = 2$

Mass locations	Mass Intensity	Frequencies		
		1	2	3
η =0.2, η =0.8	0.2	5,1788	6,7932	9,1456
	0.5	5,1719	6,7621	9,1456
	1	5,1607	6,7086	9,1456
	2	5,1381	6,5919	9,1213
η =0.4, η =0.6	0.2	5,1711	6,8064	9,1456
	0.5	5,1532	6,7957	9,1456
	1	5,1234	6,7774	9,1456
	2	5,0643	6,7400	9,1456
$\eta = 1/3, \eta = 2/3$	0.2	5,1738	6,7983	9,1456
	0.5	5,1595	6,7751	9,1456
	1	5,1362	6,7356	9,1456
	2	5,0897	6,6518	9,1456

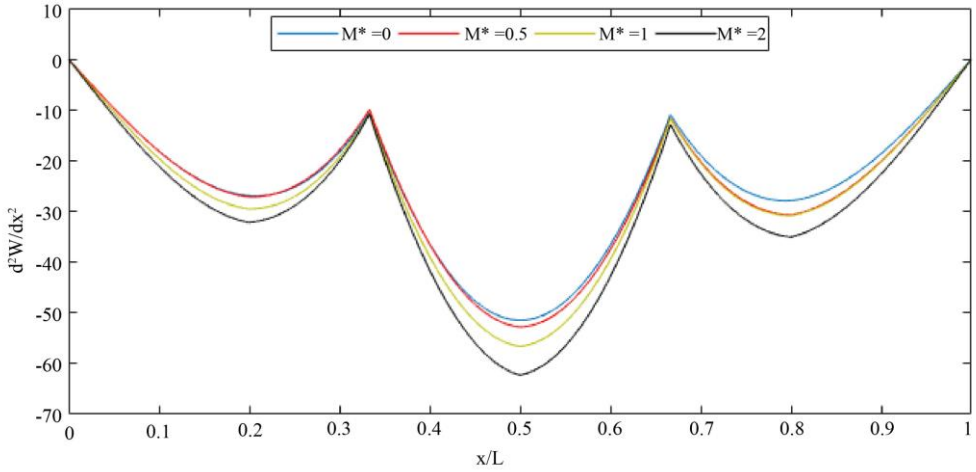

Fig. 7 Curvatures of a cable-stayed beam carrying three concentric masses with various mass magnitudes

Table 7. The frequencies of the beam, subjected to different thermal loads, are supported by a single concentric mass in the middle with a magnitude of $M = 0.5$

Mode	Thermal load			
	$\Delta T = 50\ K$	$\Delta T = 100\ K$	$\Delta T = 150\ K$	$\Delta T = 200\ K$
1	8,5889	9,2984	9,8367	10,1969
2	9,8662	10,7167	11,1553	11,6635
3	11,7224	12,6450	13,2283	13,6250

Table 8. The frequencies of the beam subjected to different thermal loads, supported by a single concentric mass in the middle with magnitudes of $M_1 = M_3 = 2$ and $M_2 = 0$

Mode	Thermal load			
	$\Delta T = 50\ K$	$\Delta T = 100\ K$	$\Delta T = 150\ K$	$\Delta T = 200\ K$
1	8,5671	9,2637	9,8119	10,1716
2	9,7503	10,5872	11,1395	11,5215
3	11,5937	12,5165	13,0750	13,5855

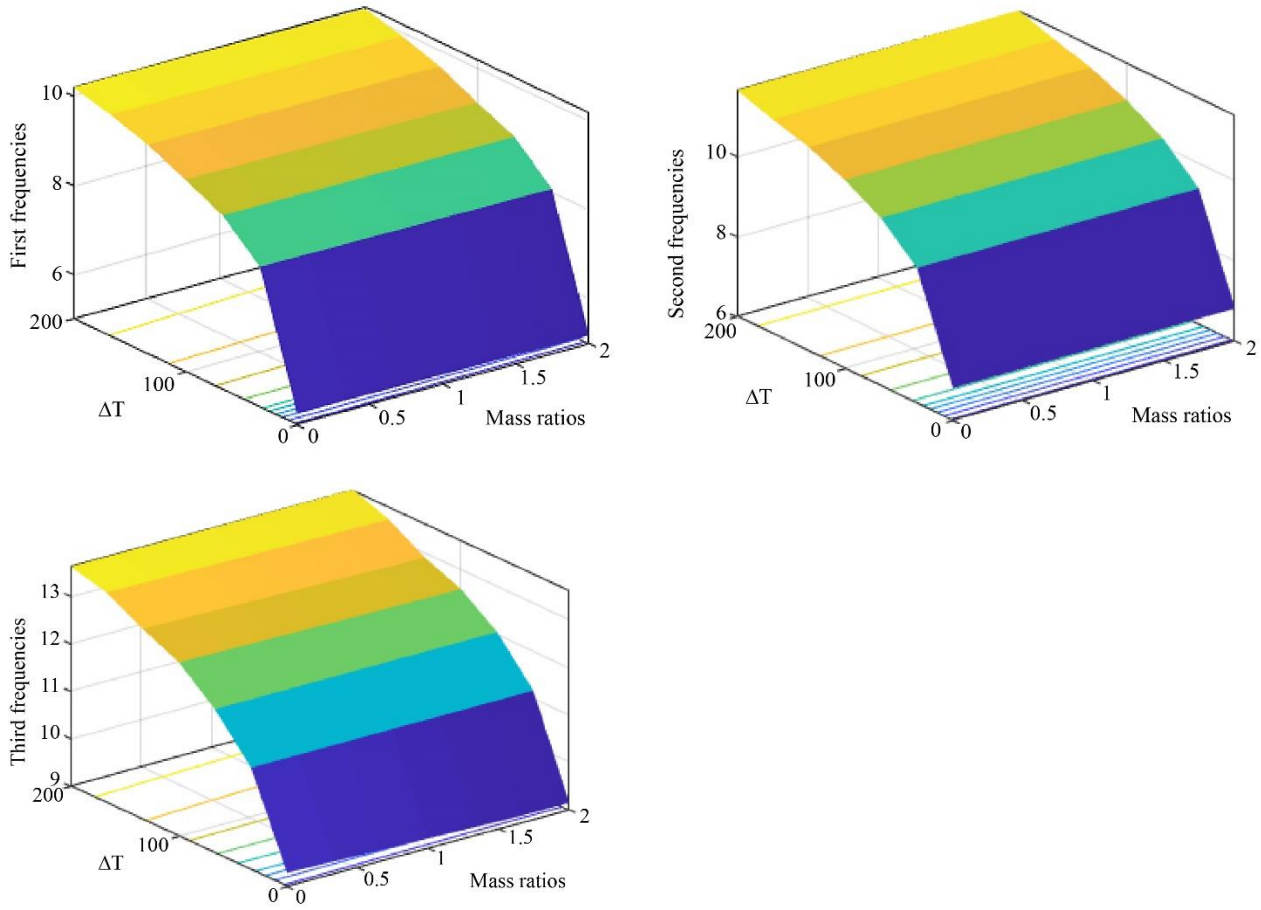

Fig. 8 The variation of the first three dimensionless natural frequencies of a suspended beam as a function of the dimensionless mass ratio and the thermal load ΔT

4. Conclusion

The study delves into the dynamics of transverse vibrations in a stayed cable system when exposed to varying thermal loads and carrying concentrated masses positioned at different points along its length.

The analysis begins by meticulously establishing boundary and continuity conditions at the junctions where the beam interfaces with the cable and at locations where the masses are attached, ensuring the structural integrity and the realistic simulation of physical behaviors.

To tackle the complexity of the system, the Newton-Raphson method, a robust numerical technique, is employed within the MATLAB environment. This iterative approach facilitates the efficient resolution of the nonlinear equations that describe the system's behavior under dynamic loads. The investigation reveals that thermal loading plays a pivotal role in influencing the natural frequencies of the beam. As thermal loads escalate, there is a corresponding increase in the natural frequencies, suggesting a stiffening effect on the cable system due to the temperature rise. Moreover, the study underscores the variability in the system's response introduced by the concentrated masses. The frequency and amplitude of the vibrations are found to be sensitive not only to the magnitude of the masses but also to their specific placements along the cable. These insights could prove invaluable for designing and optimizing cable-stayed structures in environments where thermal effects are significant, guiding engineers in making informed decisions about material selection, structural configuration, and mass distribution to achieve desired vibrational characteristics.

References

[1] Yunyue Cong et al., "Modeling, Dynamics, and Parametric Studies of a Multi-Cable-Stayed Beam Model," *Acta Mechanica*, vol. 231, pp. 4947–4970, 2020. [CrossRef] [Google Scholar] [Publisher Link]

[2] Y. Fujino, P. Warnitchai, and B.M. Pacheco, "An Experimental and Analytical Study of Autoparametric Resonance in a 3DOF Model of Cable-Stayed-Beam," *Nonlinear Dynamics*, vol. 4, pp. 111–138, 1993. [CrossRef] [Google Scholar] [Publisher Link]

[3] P. Warnitchai, Y. Fujino, and T. Susumpow, "A Non-Linear Dynamic Model for Cables and Its Application to a Cable-Structure System," *Journal of Sound and Vibration*, vol. 187, no. 4, pp. 695–712, 1995. [CrossRef] [Google Scholar] [Publisher Link]

[4] Yong Xia, and Yozo Fujino, "Auto-Parametric Vibration of a Cable-Stayed-Beam Structure under Random Excitation," *Journal of Engineering Mechanics*, vol.132, no. 3, 2006. [CrossRef] [Google Scholar] [Publisher Link]

[5] Xiaoyang Su et al., "Dynamic Analysis of the in-Plane Free Vibration of a Multi-Cable-Stayed Beam with Transfer Matrix Method," *Archive of Applied Mechanics*, vol. 89, pp. 2431–2448, 2019. [CrossRef] [Google Scholar] [Publisher Link]

[6] Hui Li et al., "Vibration Control of Stay Cables of the Shandong Binzhou Yellow River Highway Bridge Using Magnetorheological Fluid Dampers," *Journal of Bridge Engineering*, vol. 12, no. 4, pp. 401–409, 2007 . [CrossRef] [Google Scholar] [Publisher Link]

[7] M.H. El Ouni, N. Ben Kahla, and A. Preumont, "Numerical and Experimental Dynamic Analysis and Control of a Cable Stayed Bridge under Parametric Excitation," *Engineering Structures*, vol. 45, pp. 244–256, 2012. [CrossRef] [Google Scholar] [Publisher Link]

[8] Rujin Ma, Xinzhong Chen, and Airong Chen, "Effect of Cable Vibration on Aerostatic Response and Dynamics of a Long Span Cable-Stayed Bridge," *New Horizons and Better Practices*, pp. 1–10, 2012. [CrossRef] [Google Scholar] [Publisher Link]

[9] Vincenzo Gattulli et al., "One-to-Two Global-Local Interaction in a Cable-Stayed Beam Observed Through Analytical, Finite Element and Experimental Models," *International Journal of Non-Linear Mechanics*, vol. 40, no. 4, pp. 571–588, 2005. [CrossRef] [Google Scholar] [Publisher Link]

[10] Vincenzo Gattulli, Marco Lepidi, and A. Paolone, "A Parametric Analytical Model For Non-Linear Dynamics in Cable-Stayed Beam," *Earthquake Engineering & Structural Dynamics*, vol. 31, no. 6, pp. 1281–1300, 2002. [CrossRef] [Google Scholar] [Publisher Link]

[11] Vincenzo Gattulli, and Marco Lepidi, "Localization and Veering in the Dynamics of Cable-Stayed Bridges," *Computers & Structures*, vol. 85, no. 21–22, pp. 1661–1678, 2007. [CrossRef] [Google Scholar] [Publisher Link]

[12] Vincenzo Gattulli, and Marco Lepidi, "Nonlinear Interactions in the Planar Dynamics of Cable-Stayed Beam," *International Journal of Solids and Structures*, vol. 40, no. 18, pp. 4729–4748, 2003. [CrossRef] [Google Scholar] [Publisher Link]

[13] Christos Aloupis, Michael J. Chajes, and Harry W. Shenton III, "Damage Identification in Cable-Stayed Bridges based on the Redistribution of Dead and Thermal Loads," *Engineering Structures*, vol. 284, 2023. [CrossRef] [Google Scholar] [Publisher Link]

[14] Wen-Ming Zhang et al., "Analytical Study on Free Vertical and Torsional Vibrations of Two- and Three-Pylon Suspension Bridges via D," *Structural Engineering and Mechanics*, vol. 76, no. 3, pp. 293-310, 2020. [CrossRef] [Google Scholar] [Publisher Link]

[15] A. Cunha, E. Caetano, and R. Delgado, "Dynamic Tests on Large Cable-Stayed Bridge," *Journal of Bridge Engineering*, vol. 6, no. 1, pp. 54–62, 2001. [CrossRef] [Google Scholar] [Publisher Link]

[16] Wei-XinRen, Xue-Lin Peng, and You-Qin Lin, "Experimental and Analytical Studies on Dynamic Characteristics of a Large Span Cable-Stayed Bridge," *Engineering Structures*, vol. 27, no. 4, pp. 535–548, 2005. [CrossRef] [Google Scholar] [Publisher Link]

[17] Ahmed M. Abdel-Ghaffar, and Magdi A. Khalifa, "Importance of Cable Vibration in Dynamics of Cable-Stayed Bridges," *Journal of Engineering Mechanics*, vol. 117, no. 11, pp. 2571–2589, 1991. [CrossRef] [Google Scholar] [Publisher Link]

[18] Aly S. Nazmy, and Ahmed M. Abdel-Ghaffar, "Effects of Ground Motion Spatial Variability on the Response of Cable-Stayed Bridges," *Earthquake Engineering & Structural Dynamics*, vol. 21, no. 1, pp. 1–20, 1992. [CrossRef] [Google Scholar] [Publisher Link]

[19] Yunyue Cong, Houjun Kang, and Tieding Guo, "Analysis of in-plane 1:1:1 Internal Resonance of a Double Cable-Stayed Shallow Arch Model with Cables' External Excitations," *Applied Mathematics and Mechanics*, vol. 40, pp. 977-1000, 2019. [CrossRef] [Google Scholar] [Publisher Link]

[20] John C. Wilson, and Wayne Gravelle, "Modelling of a Cable-Stayed Bridge for Dynamic Analysis," *Earthquake Engineering & Structural Dynamics*, vol. 20, no. 8, pp. 707–721, 1991. [CrossRef] [Google Scholar] [Publisher Link]

[21] Mohammad Rafiee, Jie Yang, and Sritawat Kitipornchai, "Large Amplitude Vibration of Carbon Nanotube Reinforced Functionally Graded Composite Beams with Piezoelectric Layers," *Composite Structures*, vol. 96, pp. 716–725, 2013. [CrossRef] [Google Scholar] [Publisher Link]

[22] H. Asadi et al., "An Analytical Approach for Nonlinear Vibration and Thermal Stability of Shape Memory Alloy Hybrid Laminated Composite Beams," *European Journal of Mechanics - A/Solids*, vol. 42, pp. 454–468, 2013. [CrossRef] [Google Scholar] [Publisher Link]

[23] Ali Dini, Abbas Zandi-Baghche-Maryam, and Mahmoud Shariati, "Effects of Van Der Waals Forces on Hygro-Thermal Vibration and Stability of Fluid-Conveying Curved Double-Walled Carbon Nanotubes Subjected to External Magnetic Field,"*Physica E: Low-dimensional Systems and Nanostructures*, vol. 106, pp. 156-169, 2019. [CrossRef] [Google Scholar] [Publisher Link]

[24] Farajollah Zare Jouneghani, Rossana Dimitri, and Francesco Tornabene, "Structural Response of Porous FG Nanobeams Under Hygro-Thermo-Mechanical Loadings," *Composites Part B: Engineering*, vol. 152, pp. 71-78, 2018. [CrossRef] [Google Scholar] [Publisher Link]

[25] D.Q. Cao et al., "Modeling and Analysis of the in-Plane Vibration of a Complex Cable-Stayed Bridge," *Journal of Sound and Vibration*, vol. 331, no. 26, pp. 5685–5714, 2012. [CrossRef] [Google Scholar] [Publisher Link]